

Stable Polymeric Microballoons as Multifunctional Device for Biomedical Uses: Synthesis and Characterization

Francesca Cavalieri, Ali El Hamassi, Ester Chiessi, and Gaio Paradossi*

Department of Chemical Sciences and Technologies. University of Rome "Tor Vergata" and INFN, Via della Ricerca Scientifica, 00133 Rome, Italy

Received February 1, 2005. In Final Form: July 7, 2005

Gas filled hollow microparticles, i.e., microbubbles and microballoons, are soft matter devices used in a number of diverse applications ranging from protein separation and purification in food science to drilling technology and ultrasound imaging. Aqueous dispersions of these mesoscopic systems are characterized by the stabilization of the air/water interface by a thin shell of phospholipid bilayer or multilayers or by a denatured and cross-linked proteic matrix. We present a study of a type of microballoons based on modified poly(vinyl alcohol), PVA, a synthetic biocompatible polymer, with new structural features. A cross-linking reaction carried out at the air/water interface provides polymeric air-filled microbubbles with average dimensions depending on the reaction temperature. Characterization of diameters and shell thicknesses for microbubbles obtained at different temperatures has been carried out. Conversion to solvent-filled hollow microcapsules is possible by soaking microbubbles in dimethyl sulfoxide. Microcapsules permeability to fluorescent labeled dextran molecular weight standards was correlated to the mesh size of the polymer network of the shell. Microbubbles were covalently grafted under very mild conditions with β -cyclodextrin and poly-L-lysine with a view to assay the capability of the device for delivery of hydrophobic drugs or DNA. PVA based microballoons show a remarkable shelf life of several months, their external surface can be decorated with many biologically relevant molecules. These features, together with a tested biocompatibility, make them attractive candidates for use as multifunctional device for diagnosis and therapeutic purposes, i.e., as ultrasound reflectors in ecographic investigation and as drug platforms for in situ sonoporation.

Introduction

Colloidal hollow microparticles are traps for gases or liquids. Gas microbubbles based on surfactants (colloidal gas aphans)¹ are described in the literature for having distinctive features as large interfacial area, relatively high stability, easy separation from the bulk medium, and flow properties close to those of water. Such properties have suggested a number of applications in diverse fields as in food technology (protein recovery),^{2,3} in heat and mass transfer processes, and in drilling engineering. A remarkable property of gas microbubbles is their efficiency as reflectors in ultrasound imaging,⁴ a nowadays established diagnostic method. In this respect, microbubbles are the main devices used for ecographic investigations and are obtained with different kinds of materials and procedures: air-filled denatured human albumin, gaseous SF₆/phospholipids, and perfluoropropane/liposomes microbubbles.⁵ These ultrasound enhancers are commercially available. Despite the interest raised by such systems, the characterization of gas microbubble structures is still lacking and factors controlling their morphology and stability are not completely cleared out.

Efficacy in ultrasound backscattering requires the microbubbles to have an average diameter of few microns with a controlled size distribution, long time persistence in the blood stream, low gas core solubility and diffusion, suitable shell thickness, and elasticity for controlling ultrasound damping behavior.

In recent years, research aimed at more efficient ultrasound contrast agents has produced new marketed products but did not exhausted new and more demanding requirements to be found in next generation ultrasound imaging devices. One of the requisites sought in a multifunctional ecographic contrast agent is the tailoring of the surface chemical properties for specific tissue targeting.⁶ In principle, this can be done by decorating the microbubble surface with suitable selective targeting ligands, increasing the affinity of the microbubbles surface toward the tissues to be monitored. Image reconstruction of specific tissues targeted by microbubbles can be envisaged by using nonlinear response of microbubbles to ultrasound irradiation. Most of the studies carried out on echo-contrast agents were limited to the linear region of the backscattering where the ultrasound amplitude is low. For moderately higher output power, the nonlinear scattering behavior of the microbubbles shows sharp pressure peaks in the compression stage producing second harmonic oscillations.⁷ This effect can be used for differentiating tissues from the contrast agent imaging.

Another important issue related to the multifunctionality of the microbubbles is the possibility to use such devices as drug delivery systems.^{8–11} In this respect a significant asset of microbubbles is their injectability compared to oral administration performed with tablets or hydrogels. In this way, the carrier, i.e., the microbubbles, is able to arrive through the systemic circulation to the

* Corresponding author. E-mail: paradossi@stc.uniroma2.it.

(1) Jauregi, P.; Mitchell, G. R.; Varley, J. *AIChE J.* **2000**, *46*, 24–36.

(2) Jauregi, P.; Varley, J. *Trends Biotechnol.* **1999**, *17*, 389–395.

(3) Fuda, E.; Jauregi, P.; Pyle, D. L. *Biotechnol. Prog.* **2004**, *20*, 514–525.

(4) Schutt, E. G.; Klein, D. H.; Mattrey, R. M.; Riess, J. G. *Angew. Chem., Int. Ed.* **2003**, *42*, 3218–3235.

(5) Feinstein, S. B. *Am. J. Physiol. Heart Circ. Physiol.* **2004**, *287*, H450–H457.

(6) Lindner, J. R. *Am. J. Cardiol.* **2002**, *90*, 72J–80J.

(7) Chang, P. P. *IEEE Trans. Ultrason., Ferroelect., Freq. Contr.* **2001**, *48*, 161–170.

(8) Klibanov, L. *Adv. Drug Delivery Rev.* **1999**, *37*, 139–157.

(9) Morawski, A. M.; Lanza, G. A.; Wickline, S. A. *Curr. Opin. Biotechnol.* **2005**, *16*, 89–92.

(10) Riess, J. G. *Curr. Opin. Colloid Interface Sci.* **2003**, *8*, 259–266.

(11) Unger, E. C.; Matsunaga, T. O.; McCreery, T.; Schumann, P.; Sweitzer, R.; Quigley, R. *Eur. J. Radiol.* **2002**, *42*, 160–168.

target tissue with *in situ* release of chemically attached or encapsulated drug by in-resonance ultrasonic bubbles cavitation¹² as recently shown by Lindner.¹³ However, loading of microbubbles with therapeutic agents requires a cargo space available in the shell which is relatively small in conventional microbubbles. Thicker polymeric shells can satisfy such requirement and in the meantime confer a higher stability to the microbubbles. A patent claiming contrast agents based on biodegradable polymeric materials selected from polysaccharides, polypeptides, polylactides, polyglycolides, polyanhydrides, and polyglutamates appeared recently.^{14a,b} Microsized capsules were fabricated by polystyrene beads self-assembling and inflated by osmotic pressure effect due to the presence of poly-L-lysine in the capsule core.¹⁵ Liu et al.¹⁶ recently reported on stable polymeric nanoballoons obtained by cross-linking polymerization of liposomes. Hollow nanosized polyelectrolyte capsules are a popular example of nanoassembly found in the literature.^{17,18} The build up of alternate oppositely charged polyelectrolyte layers on a charged spherical template followed by its calcination or dissolution yields hollow nanoscaled particles.

Our aim is the formulation of devices acting as ultrasound scattering enhancers using as starting material poly(vinyl alcohol), PVA, a synthetic polymer with good biocompatibility properties,^{19,20} that matches some of the requirements imposed by a multifunctional use of the device. We have obtained aqueous suspensions of polymeric microballoons by using a method that differs from those described in the literature. In our case, air is entrapped in a polymer shell obtained by chemically cross-linking, at high sheer rate, modified PVA. Interfacial polymer networking was carried out by an acetalization reaction of aldehydic end groups born on PVA telechelic chains. The microballoon suspension, separated by flotation and stocked at room temperature in water, showed a shelf life of many months. In our opinion these type of microballoons could be considered as a potential candidate for ultrasound investigations.

Considering the interaction of microbubbles with ultrasounds,^{21,22} the formulation of a new class of mesoscopic systems functioning simultaneously as echo-contrast and drug delivery agents can be assessed. The echogenic properties, as the pressure threshold at which these microbubbles undergo inertial cavitation, are under investigation, nevertheless chemical and physical properties of PVA based microbubbles need to be well characterized. In this context, loading and release of high and low molecular weight drug molecules can be envisaged, tuning the surface chemical properties by suitable functionalization methods. Therefore, we have modified with different molecules the microbubbles surface as a preliminary

step for a potential use of these systems in efficient tissue targeting and controlled drug release function. Moreover an alternative approach for the production of hollow microcapsules has been devised by exploiting the ability of PVA based microbubbles to modulate their wall permeability by changing solvent. Hollow microcapsule may also have applications in biology and medicine as microcontainers and microreactors for drug enzymes, DNA, and other bioactive molecules.²³

In this work, we present the synthesis and characterization study of PVA based microbubbles and microcapsules derived from interfacial cross-linking of telechelic PVA via acetalization. Polymeric shell has been studied in terms of permeability properties and chemically modified for further development of these systems.

Experimental Section

Materials. Poly(vinyl alcohol) was a Sigma product. Number average molecular weight determined by membrane osmometry was $30\ 000 \pm 5\ 000$ g/mol. Weight average molecular weight, determined by static light scattering, was $70\ 000 \pm 10\ 000$ g/mol.

Dimethyl sulfoxide, acetone, sodium periodate, and inorganic acids and bases, used for telechelic PVA preparation and microballoons synthesis and modifications, were RPE products from Carlo Erba.

Fluorescein isothiocyanate isomer I, FITC, Rhodamine B isothiocyanate, RBTC, and 5-(4,6-dichlorotriazinyl)aminofluorescein, DTAF, were purchased from Fluka.

Fluorescein isothiocyanate-dextran T20 with a number average molecular weight of 20 000 and a labeling density of 0.004 mol of FITC/mol of glucose was supplied by Sigma. Dextran T70 with a number average molecular weight of 70 000 daltons was purchased from Amersham Pharmacia Biotech.

All chemicals were reagent grade and used without further purification.

Water was Milli-Q purity grade ($18.2\ M\Omega\cdot\text{cm}$), produced with a deionization apparatus (PureLab) from USF.

Methods. *Synthesis of PVA Coated Microballoons.* Synthesis of telechelic PVA was previously described in the literature.^{23,24} Stable PVA coated microballoons (air-filled) were prepared by interface cross-linking telechelic PVA. Vigorous stirring at room temperature for 3 h of 2% telechelic PVA aqueous solution (100 mL) at pH 2.50 by an Ultra-Turrax T-25 at 8000 rpm equipped with a Teflon coated tip, generated a fine foam of telechelic PVA acting both as colloidal stabilizer and air bubble coating agent. The cross-linking reaction was stopped by neutralizing the mixture. Floating microballoons were separated from solid debris and extensively dialyzed against water. An aqueous suspension of microballoons was obtained and used for further chemical modification. This procedure was carried out at room temperature and at 5 °C in the presence of hydrochloric or sulfuric acid as catalyst for the cross-linking reaction.

Characterization of PVA Microballoons. Particle size distribution was evaluated by dynamic light scattering, DLS, matching the density of particles to that of the medium. 80/20 and 87/13 (v/v) water/acetone mixtures were used as density matching liquids. For these measurements, a BI-200SM goniometer (Brookhaven Instrument Co.), equipped with a laser source at 532 nm, was used. The correlation functions were analyzed with CONTIN algorithm.

FITC and RBTC were used for fluorescent labeling of the microballoons. Fluorescent dyes (10 μM) were added into the suspension. Floating particles were washed by re-suspending them in MilliQ water several times. Confocal images were acquired by a confocal laser scanning microscope (CLSM), Nikon PCM 2000 (Nikon Instruments), a compact laser scanning microscope based on a galvanometer point-scanning mechanism, a single pinhole optical path, and multi-excitation module

- (12) Miller, D. L.; Pislaru, S. V.; Greenleaf, J. F. *Somat. Cell. Mol. Genet.* **2002**, *27*, 115–134.
- (13) Senter, P. D.; Kopecek, J. *Mol. Pharm.* **2004**, *1*, 395–398.
- (14) (a) Bichon, D.; Bussat, P.; Schenider, M. U.S. Patent, 6,200,548, 2001. (b) Fritzsche, T.; Hilmann, J.; Kampfe, M.; Muller, N.; Schobel, C.; Siegert, J. *J. Invest. Radiol.* **1990**, *25*, S160–S161.
- (15) Gordon, D. V.; Chen, X.; Hutchinson, J. W.; Bausch, A. R.; Marquez, M.; Weitz, D. A. *J. Am. Chem. Soc.* **2004**, *126*, 14117–14122.
- (16) Liu, S.; O'Brien, D. F. *J. Am. Chem. Soc.* **2002**, *124*, 6037–6042.
- (17) Caruso, F. *Adv. Mater.* **2001**, *13*, 11–12.
- (18) Caruso, F.; Caruso, R. A.; Mohwald, H. *Science* **1998**, *282*, 1111–1114.
- (19) DeMerlis, C. C.; Schoneker, D. R. *Food Chem. Toxicol.* **2003**, *41*, 319–326.
- (20) Kelly, C. M.; DeMerlis, C. C.; Schoneker, D. R.; Borzelleca, J. F. *Food Chem. Toxicol.* **2003**, *41*, 719–727.
- (21) Wei, K.; Skyba, D. M.; Firsche, C.; Jayaweera, A. R.; Lindner, J. R.; Kaul, S. J. *Am. Coll. Cardiol.* **1997**, *29*, 1081–1088.
- (22) Giesecke, T.; Hyynen, K. *Ultrasound Med. Biol.* **2003**, *29*, 1359–1365.

- (23) Gleb, B.; Mohwald, S.; Mohwald, H. In *Colloids and Colloid Assemblies: Synthesis, Modification, Organization and Utilization of Colloid Particles*; Caruso, F., Ed.; Wiley-VCH: Weinheim, Germany, 2004; pp 561–580.

- (24) Paradossi, G.; Cavalieri, F.; Chiessi, E.; Ponassi, V.; Martorana, V. *Biomacromolecules* **2002**, *3*, 1255–1262.

equipped with Spectra Physics Ar-ion laser (488 nm, 514 nm) and He-Ne laser (543.5 nm) sources. A 60x/1.4 oil immersion objective was used for the observations. Tests carried out by measuring giant liposome shells provided a value of $0.25\text{ }\mu\text{m}$ for instrumental resolution. Shell thickness of fluorescent labeled microparticles were measured as the full width at half-maximum of the fluorescence intensity profile.

Conversion of Telechelic PVA Microballoons into Microcapsules. PVA microballoons were converted into solvent filled microcapsules by equilibrating an aqueous suspension in dimethyl sulfoxide, DMSO. The replacement of air in microballoons cavities by DMSO was observed by CLSM, marking the organic phase with fluoresceine and checking that an equal fluorescence intensity background was present inside and outside the rhodamine labeled microparticles.

Evaluation of Microballoons Permeability to Dextrans by CLSM. Labeling of dextran T70 by DTAF fluorescent probe was carried out as follows: 10 mg of DTAF were dissolved in 1.5 mL of 0.1 M borate buffer (pH 9) and added to 30 mg of dextran T70 dissolved in 1.5 mL of the same buffer. The mixture was gently stirred overnight at room temperature. DTAF labeled dextran was separated from free DTAF by extensive dialysis (cutoff 12,000 g/mol) against MilliQ water. Labeling density of 0.019 mol of DTAF/mol of glucose was determined by spectrophotometer absorption at 492 nm using an extinction coefficient of 83 000 $\text{M}^{-1}\text{ cm}^{-1}$ for DTAF.

Microballoons and microcapsules were exposed overnight to DTAF-dextran T70 and to FITC-dextran T20 and washed with MilliQ water. Microparticles permeability was monitored by CLSM visualization and the extent of permeation was evaluated by analysis of the fluorescence intensity profile.

ζ -Potential Measurements. ζ -Potential measurements were carried out with a ζ -potential particle analyzer (Brookhaven, New York). 1.5 mL of particle dispersion at a concentration of 1 g/L was loaded in the measuring cell using 0.01 M KCl as supporting electrolyte. Measurements were the average of 6 repetitions. ζ -Potential values of $-4.7 \pm 0.6\text{ mV}$ were found for all types of PVA microbubbles studied in this work.

Preparation of β -Cyclodextrin Functionalized Microbubbles. Coupling of β -cyclodextrin to the microballoon surface was achieved by acetalization reaction between microbubbles suspension (0.8 mg/mL) and a 0.02 M β -cyclodextrin aqueous solution. After incubation for 24 h at 25 °C and pH 3 the resulting mixture was neutralized and extensively dialyzed against water in order to remove free β -cyclodextrin. ^1H NMR spectrum was recorded on a Bruker 400 MHz on D_2O suspension of microbubbles.

Preparation of Poly-L-lysine Functionalized Microbubbles. A total of 10 mL of aqueous suspension of microbubbles (0.8 mg/mL) was incubated with 3 mg/mL solution of poly-L-lysine (MW 7,500 g/mol) at room temperature and pH 5. After 24 h, microbubbles were extensively dialyzed to remove unreacted poly-L-lysine. CD spectra were recorded in the range 200–250 nm by using a quartz cell (1 mm) with a JASCO J600 spectrometer equipped with a thermoregulated cell compartment.

Results and Discussion

Characterization of the PVA Microballoons Prepared at Room Temperature. Recently we have shown a synthetic route to obtain uniform, wall-to-wall hydrogels by acetalization of telechelic PVA carrying carbonyls as end-groups.^{24,25} Here this approach is used to obtain air-filled microspheres by performing the acetalization at the air–water interface under high shear conditions. The air filled hollow particles were separated by flotation from PVA debris precipitated at the bottom of the reaction flask. Both components were observed by means of confocal microscopy. The scanning of focused equatorial slice of rhodamine labeled microballoon shells and the fluorescence intensity profile, measured across the microparticle, allowed an evaluation of the particle dimensional char-

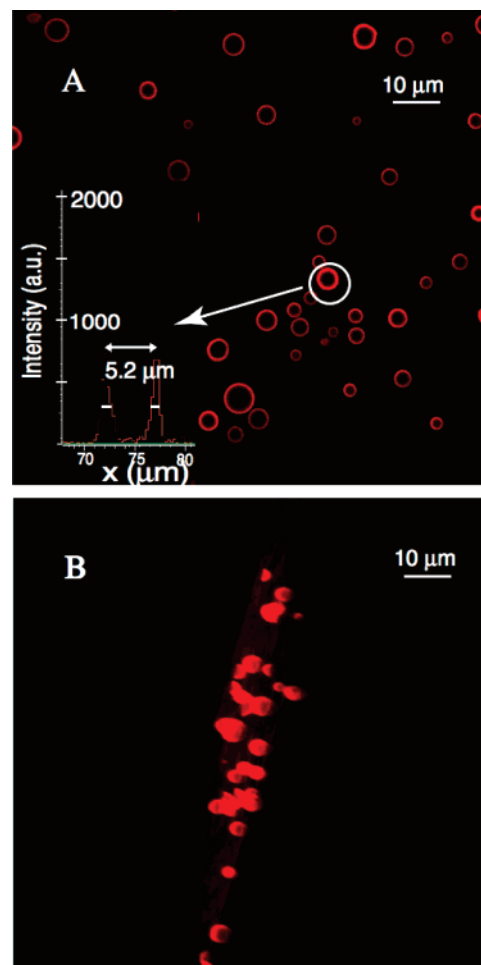


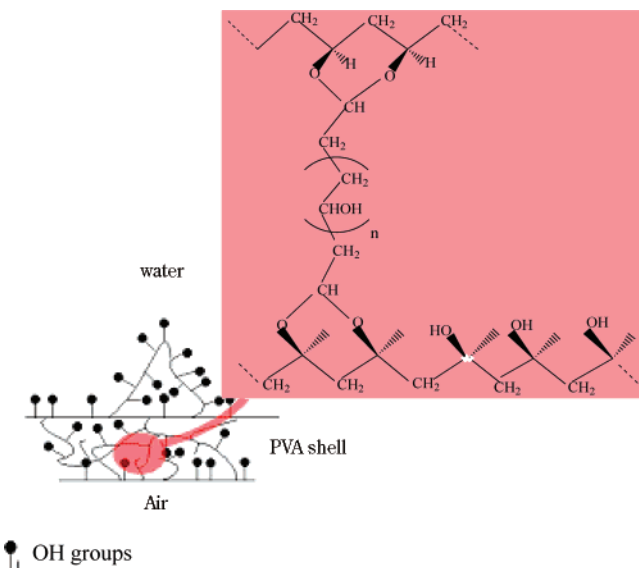
Figure 1. (A) 2D CLSM image of rhodamine isothiocyanate labeled microballoons prepared at room temperature. Insert: fluorescence intensity profile acquired for the size and shell thickness determination. (B) 3D CLSM image.

acteristics. In Figure 1A, the circled particle has a diameter of $5.2\text{ }\mu\text{m}$ and a shell thickness of $0.9\text{ }\mu\text{m}$, estimated from the fluorescent contour showed in the insert.

In Figure 1B, the 3D image reconstruction confirms the spherical geometry of the microballoons. Confocal microscopy analysis of this microbubbles sample on a statistically representative number of 200 observations yielded a dimension distribution with a mean diameter of $5\text{ }\mu\text{m}$ (standard deviation $1\text{ }\mu\text{m}$) and an average shell thickness of $0.90\text{ }\mu\text{m}$. The standard deviation of the shell thickness is equal to the instrumental resolution of $0.25\text{ }\mu\text{m}$, not allowing a statistical evaluation of the distribution spread. Microballoon average diameters and size polydispersity were also investigated by dynamic light scattering experiments (DLS). Buoyancy of microbubbles during acquisition of the correlation function was avoided by dispersing the microparticles in a water/acetone 80/20 mixture corresponding to a density of 0.9857 at room temperature. CONTIN analysis of the DLS correlation functions showed a diameter distribution centered at a mean diameter of $5\text{ }\mu\text{m}$ with a broadness (standard deviation) of $1\text{ }\mu\text{m}$.

To understand the reasons leading to the formation of microbubbles coated by a PVA shell, it should be taken into account the dual nature of this polymer. The amphiphilic nature of the PVA repeating unit is provided by the presence of hydrophilic and hydrophobic moieties represented by the hydroxyl and the aliphatic methylene groups, respectively. For these chemical features, PVA

Chart 1. Schematic Representation of the Air-polymer Shell-water Interfaces



chains in aqueous solutions form clusters of entangled chains stabilized both by hydrophobic interactions and by inter- and intramolecular hydrogen bonds. Moreover due to its surfactant behavior, PVA in water decreases the surface tension of aqueous solutions to a value of about 50 mN/m for concentrations higher than 0.5% (w/v).²⁶ In this respect, telechelic PVA shows a foaming ability under high shear stirring. The radius of the initial microbubble, R , is dictated by the surface tension γ and the pressure drop, Δp , through the Laplace–Young equation: $R = 2\gamma/\Delta p$. In the early stage of the shell formation, PVA chains will migrate from the bulk of the aqueous solution to the air–solution interface acting as a surfactant. Segregation of PVA at the surface creates the proper conditions for microbubbles stabilization. Chart 1 illustrates the behavior of PVA chains at the interface in order to minimize its free energy: aliphatic groups will arrange at the air phase and hydroxyl groups will point toward the aqueous phase. The build up of the shell is due to PVA accumulation according to Gibbs adsorption equation up to the leveling off of the surface tension with PVA concentration, and to the simultaneous formation of chemical cross-links in the shell via acetalization. Shell thickening will proceed till phase separation conditions are met. Other factors contribute to the unusual stability of PVA microballoon dispersions. The submicron cross-linked polymer shell, acting as a barrier to air escaping, ensures that the bubble is not in diffusive equilibrium with the bulk. Coagulation of microballoons is remarkably slowed by steric colloidal stabilization due to the presence of polymer chains protruding from the shell to the bulk.

PVA microballoon features can be conveniently exploited for encapsulating molecules. We have devised a procedure to convert microballoons into microcapsules by embedding the microballoons in DMSO. Evacuation of air is driven by the pressure gradient and by the increased permeability of the PVA shell in the presence of DMSO, ascribable to the better solvent quality of this organic phase for PVA than water, as it is suggested by the Flory-Huggins parameter χ values of 0.4 and 0.55, respectively. The effective air replacement was confirmed by marking the organic solvent with fluoresceine and monitoring by

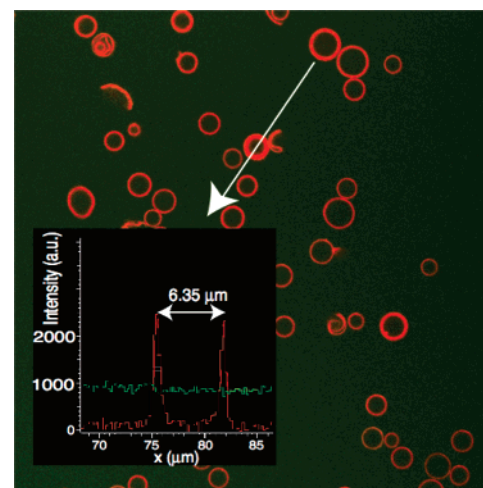
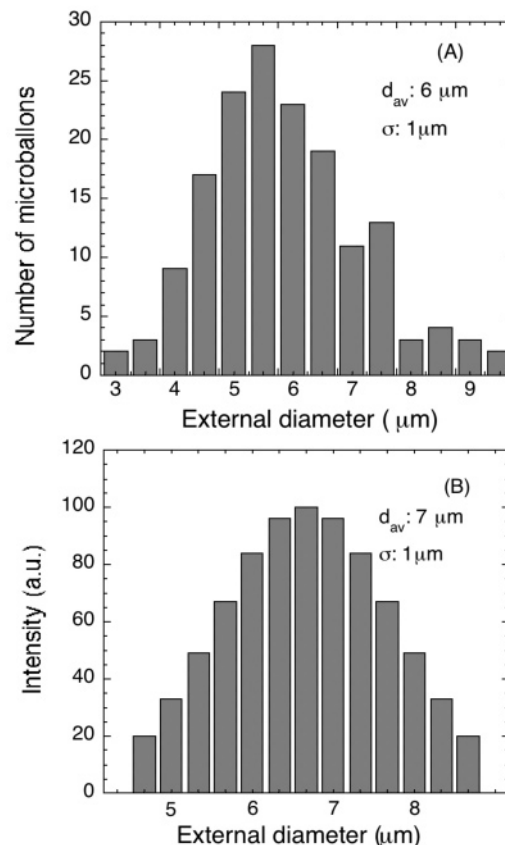


Figure 2. CLSM image of rhodamine isothiocyanate labeled microcapsules incubated with fluorescein dye. Insert: fluorescence background (green trace), rhodamine isothiocyanate fluorescence (red trace) denoting microbubble shell.



confocal microscopy an equal fluorescence intensity background throughout the particle internal cavity, as it is shown in Figure 2.

This procedure allowed the conversion of microballoons into microcapsules, and a size analysis was carried out by both dynamic light scattering and confocal laser scanning microscopy.

In Figure 3, panels A and B, the DLS and CLSM external diameters distributions of the PVA based microcapsules are shown. Mean diameters of 6 ± 1 and of $7 \pm 1 \mu\text{m}$, respectively, are found indicating a swelling effect on the overall dimensions of the particle, confirming the better solvation properties of DMSO.

Table 1. Structural Parameters of PVA Microbubbles and Microcapsules Obtained at Room Temperature

	external diameter, μm	internal diameter, μm	shell thickness, μm
microbubbles	$5^a \pm 1$	$3^a \pm 1$	$0.90^a \pm 0.25^c$
	$5^b \pm 1$		
microcapsules	$6^a \pm 1$	$4^a \pm 1$	$1.00^a \pm 0.25^c$
	$7^b \pm 1$		

^a Confocal laser scanning microscopy. ^b Dynamic light scattering. ^c Confocal microscope resolution.

Table 2. Structural Parameters of PVA Microbubbles and Microcapsules Obtained at 5 °C

	external diameter, μm	internal diameter, μm	shell thickness, μm
microbubbles	$3.0^a \pm 0.8$	$1.6^a \pm 0.8$	$0.70^a \pm 0.25^c$
	$3^b \pm 1$		
microcapsules	$4^a \pm 1$	$3^a \pm 1$	$0.60^a \pm 0.25^c$
	$5.0^b \pm 0.5$		

^a Confocal laser scanning microscopy. ^b Dynamic light scattering. ^c Confocal microscope resolution.

According to CLSM image analysis, the shell thickness remains unchanged in the conversion to microcapsules. The statistical evaluation of the shell thickness distribution yielded an average value of $1.0 \mu\text{m}$ as summarized in Table 1. The obtainment of PVA based microcapsules could open new perspectives in the potential use of such systems as injectable drug delivery devices, where the pharmacologically active molecule can be loaded during the conversion to microcapsules by dissolution of the drug in a “good solvent” medium for PVA and released by dispersing the microcapsules in water.

Another remarkable feature of microbubbles is their physical and chemical stability which allow a storage period of months at room temperature in distilled water. Commercially available contrast agent enhancers do not possess such a prolonged shelf life. Those based on denatured proteins are subjected to chemical or biological deterioration, whereas lipid based microbubbles are in diffusive equilibrium with the bulk with consequent escape of trapped gases in short periods.

Shelf life of PVA microbubbles is remarkably longer compared to other existing microbubbles. This feature is the results of the combined action of factors as (i) a very low permeability coefficient of PVA to most gas permeants, i.e., lower than $0.009 (\text{cm}^3 \text{ cm})/(\text{cm}^2 \text{ s Pa})$,²⁵ (ii) a steric colloidal stabilization due to the limited interpenetration of the PVA chains projecting from the surface into the solvent. A summary of the structural features of PVA microbubbles obtained at room temperature and derived microcapsules is reported in Table 1.

Characterization of the PVA Microballoons Prepared at 5 °C. Microbubble preparations based on telechelic PVA and carried out at 5 °C present remarkable differences with those obtained at room temperature in that a higher numeric density of microbubbles but with smaller dimensions is obtained. This effect can be explained in terms of a depletion of gas in water as the temperature is lowered, due to a decreased saturation level of water, with the consequent shrinking of the microbubbles.

The DLS and CLSM analysis on microbubbles obtained at 5 °C is reported in Table 2.

From DLS and CLSM on 300 observations, average diameters of $3 \mu\text{m}$ with a spread (standard deviation) of $1 \mu\text{m}$ are obtained.

An evaluation of the shell thickness carried out by a CLSM on rhodamine-labeled microballoons provided an

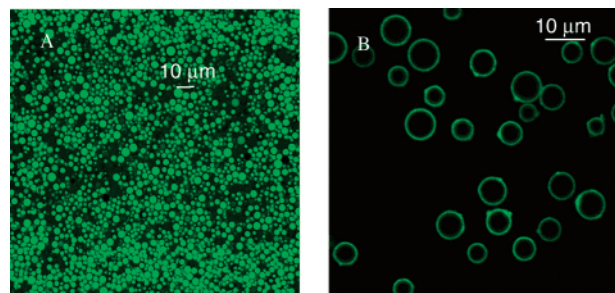


Figure 4. (A) CLSM image of microcapsules incubated for several hours in the presence of FITC-labeled dextran T20, indicating that both capsule shells and cores are accessible to this probe. (B) CLSM image of microcapsules treated with FITC-labeled dextran T70, indicating the absence of macro-molecular fluorescent probe in the microcapsule core.

average value of $0.7 \mu\text{m}$. The same considerations about the distribution spread of the microballoons prepared at room temperature apply also in this case. Conversion into microcapsules was also possible in this case by soaking the microballoons in DMSO. A swelling effect on the overall dimension of the microcapsules, shown in Table 2, was observed as well.

Information about the architecture of the polymer shell has been obtained by studying the permeation of solutions containing dextrans with different molecular weights and labeled with a fluorescent probe through the microcapsule shell. Microcapsules derived from PVA microbubbles, incubated with 20 000 g/mol FITC-labeled dextran, are rinsed with water and observed by CLSM. The permeation of the polymer shells is complete and the probe fills the core of the microcapsules. Dextran assumes in solution a random coil conformation and a 20 000 g/mol polysaccharide chain corresponds to a coil with a hydrodynamic radius of about 3.5 nm .²⁷

On the contrary, after prolonged incubation with DTAF-labeled dextran T70 with a hydrodynamic radius of 6.5 nm ,²⁸ see Figure 4 B, only a partial permeation of the shell wall is obtained as evidenced by the absence of labeled dextran in the microcapsule cavity. These findings provide an evaluation of pore size of the polymer shell, ranging between 3.5 and 6.5 nm but also suggest that the shell architecture is characterized by a cross-linking density gradient consisting of larger pores at the polymer/solution interface and smaller ones at the air/polymer interface. This uneven pore distribution can be reminiscent of the interfacial networking process leading to the build up of the microbubble shell with a higher density of telechelic PVA in the early stages of the shell formation. Bulges, visible in Figure 4B, on the microbubbles surface can be originated by an analogous process involving phase separation of polymeric material occurring during the shell formation.^{29,30}

Microbubbles numerical density and size are influenced by several reaction parameters such as the nature and concentration of the acid catalyst, reaction temperature, and polymer concentration. Tests were performed in order to sort out the role of these parameters in the obtainment of microballoons. A summary of the results is given in Table 3.

(27) Brandrup, J.; Immergut, E. H.; Grulke, E. A. *Polymer Handbook*, 4th ed.; Wiley-Interscience: New York, 1999; p VI/550.

(28) Brissova, M.; Petro, M.; Lacik, I.; Powers, A. C.; Wang, T. *Anal. Biochem.* **1996**, *242*, 104–111.

(29) Jung, M.; Robinson, B. H.; Steytler, D. C.; German, A. L.; Heenan, R. K. *Langmuir* **2002**, *18*, 2873–2879.

(30) Krafft, M. P.; Schieldknecht, L.; Maire, P.; Giulieri, F.; Schmutz, M.; Poulain, N.; Nakache, E. *Langmuir* **2001**, *17*, 2872–2877.

Table 3. Particles Concentration Dependence on Reaction Conditions

T, °C	catalyst	catalyst conc., mol/L	polymer conc., (w/v) %	reaction time (hours)	particles density $\times 10^{-7}$ (particles/mL)
25	H ₂ SO ₄	0.02	2	3	1.4
5	H ₂ SO ₄	0.02	2	3	7.0
25	HCl	0.01	2	3	0.9
5	HCl	0.01	2	3	5.6
25	H ₂ SO ₄	0.02	1	3	0
25	H ₂ SO ₄	0.02	4	3	0
25	H ₂ SO ₄	0.06	2	3	0

From these results, some considerations can be drawn: (i) sulfuric acid is a more efficient catalyst for microbubble production, as it can be expected by considering that the cross-linking reaction stabilizing the microbubble shell is an acetalization reaction, and (ii) that a lower temperature leads to the obtainment of a more concentrated particles suspension because of the more efficient foaming behavior of telechelic PVA in this condition. Polymer concentration greatly influences the microbubbles yield, as shown in Table 3. At 0.02 mol/L H₂SO₄, an optimal polymer concentration of 2% (w/v) is found. At higher polymer concentrations, the formation of PVA clusters, slowly diffusing to the air–water interface, inhibits the progressive growth of microbubble shells, whereas a polymer concentration lower than 2% provides thin shells, unable to stabilize the microbubble.

Although particles densities obtained in these trials are suitable for echo-contrast use, the measured low yield, about 4%, is a feature common in self-assembling reactions involving micron sized architectures. An even lower yield, about 0.1%, has been reported for the reaction leading to giant liposomes.³¹

Confocal microscopy investigation was carried out after solvent evaporation and consequent microballoons aggregation. In Figure 5, a lump of densely packed microballoons is shown.

Clustering is simply due to the solvent removal by evaporation. Perfect reversibility is observed when the microbubbles are diluted, since aldehydes present on the microballoon surfaces are reactive only in acidic conditions. Deformations of the polymer shells are clearly visible, indicating deformability of the balloon surface. The elasticity of the surface is under investigations as it should influence the microballoons response to ultrasound irradiations and in particular the echogenic properties of these microparticles.

Surface reactivity of microballoons is an important issue in determining the biocompatibility of this device and its derivatization. According to proton NMR investigation carried out on telechelic solution, PVA chain segments bearing terminal masked aldehyde groups are present as evidenced by signals displayed at 4.5–5.0 ppm and assigned to hemiacetal protons. Microballoons shell cross-linking entails intermolecular telechelic acetalization but leaves unreacted few aldehyde chain ends, in the form of intramolecular hemiacetal, tethered to the shell and protruding toward the solution. The presence of masked aldehyde is a contributing factor to the biocompatibility of the microballoons towards several cellular strains (to be published³²) as reactive aldehyde groups are usually cytotoxic. Moreover, this chemical feature can be conveniently used for derivatization of the microballoons surface with molecules of pharmaceutical relevance reactive to aldehydes.

(31) Akashi, K.; Miyata, H.; Ithoh, H.; Kinoshita, K. *Biophys. J.* **1998**, 74, 2973–2982.

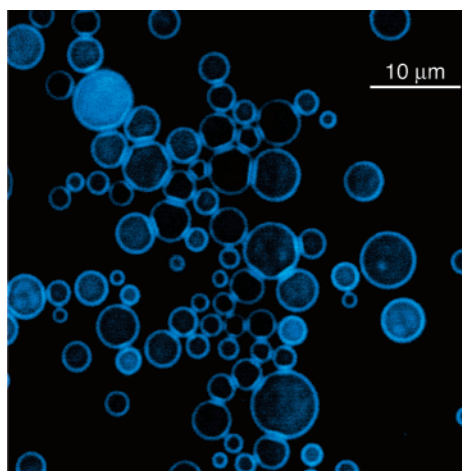


Figure 5. CLSM image of densely packed microballoons indicating shell deformation.

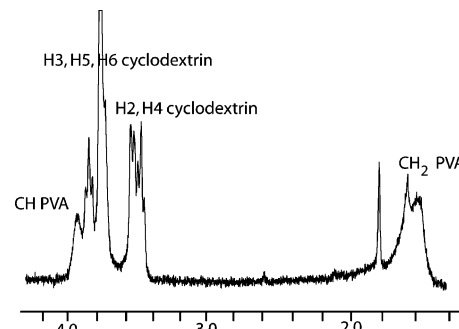


Figure 6. Proton NMR spectrum of derivatized PVA microballoons with β -cyclodextrin.

In this paper we report on the derivatization of Microballoon surfaces with two case molecules, β -cyclodextrin and poly-L-lysine, PLL. The former molecule can be used to include and deliver scarcely water soluble drugs, the latter is a model for the potential use in gene therapy of modified microballoons as drug delivery systems for oligonucleotide drugs.³³

Derivatization with β -cyclodextrin is obtained by activating at low pH the aldehyde groups masked as acetals. The coupling to the Microballoon surface occurs by means of a condensation reaction with hydroxyl groups of the saccharidic moiety. The β -cyclodextrin derivatization is indicated by the H-1 proton resonance at 3.4–4.0 ppm in the NMR spectrum (see Figure 6) of an aqueous suspension of microballoons exhaustively dialyzed against water.

The ¹H NMR spectrum of microbubbles suspension indicates the high flexibility of the chain ends covalently linked to β -cyclodextrin, as rather sharp signals were recorded for PVA backbone methine groups at 4.1 ppm and methylene groups at 1.5 ppm. Polymer chains tentacles, protruding toward the solution from the microbubbles surface, exhibit a mobility similar to that measured in solution whereas the polymer chains engaged in the build up of the shell have a much lower mobility and their relaxation decays are silent to the probed NMR time scale.

Poly-L-lysine surface decoration is carried out by means of a Schiff base coupling. A circular dichroism spectrum of a diluted aqueous suspension of PLL modified mi-

(32) Cavalieri, F.; El Hamassi, A.; Chiessi, E.; Paradossi, G.; Villa, R.; Zaffaroni, N. *Bioconjugate Chem.* **2005**, submitted.

(33) Unger, E. C.; Porter, T.; Culp, W.; Labell, R.; Matsunaga, T.; Zuttschi, R. *Adv. Drug Delivery Rev.* **2004**, 56, 1291–1314.

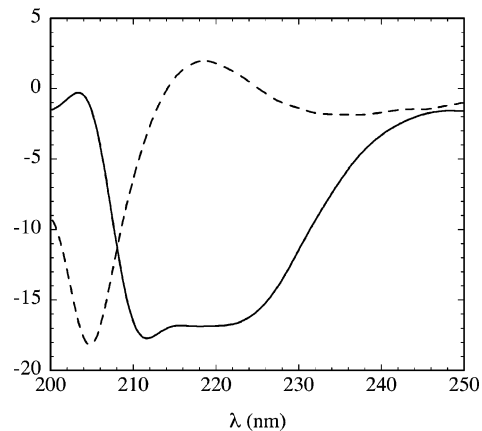


Figure 7. Circular dichroism spectra of poly-L-lysine anchored on PVA microballoons. Full line pH 12; dashed line pH 5.

microballoons, exhaustively dialyzed against water, is reported in Figure 7. The ellipticities in the 250–200 nm UV range show the typical fingerprints of the random coil and of the α helical conformations, at neutral pH and at

basic pH, respectively. The retained ability of the polypeptide to a reversible random coil \leftrightarrow α helix conformational transition indicates that the attachment of the polypeptide does not interfere with its conformational properties.

In conclusion, the synthesis and functionalization of novel PVA based microbubbles described in this work show the versatility of this mesoscopic device being able to behave as a functional gas aphon and readily transformable into microcapsule for aqueous phase confinement. The potentialities of this device, combined with a remarkable shelf life and mild preparation conditions, can be the basis for further developments of an interesting material referred as “smart microbubbles” to be used as multi-functional agent for controlled drug delivery and ultrasound diagnostics.

Acknowledgment. We acknowledge partial support for this work from the INFM FIRB Grant RBNE01XPYH. We thank Dr. F. Sonvico and Prof. A. Deriu for ζ -potential measurements.

LA050287J